

Plasma ionization and resistivity models in application to radiative properties of z-pinch

A. A. Esaulov¹, W. R. Johnson², A. S. Safronova¹, U. I. Safronova¹, V. L. Kantsyrev¹, M. E. Weller¹, and N. D. Quart³

¹University of Nevada, Reno NV 89557, USA

²University of Notre Dame, IN 46556, USA and

³Naval Research Laboratory, Washington, DC 20375, USA

(Dated: August 11, 2011)

The LTE Saha–Boltzman plasma ionization balance model and the Braginskii plasma electric resistance model are compared with the results by the suit of codes based on the average atom model, which is a quantum-mechanical version of the Temperature Dependent Thomas–Fermi Theory. The analysis is focused on low- Z Al, mid- Z Cu and higher- Z Mo plasmas in a broad ranges of electron temperature T_e and electron number density n_e . Calculations of mean ion charge by these two LTE models are verified versus the results produced by non-LTE atomic kinetic codes. The applicability of the LTE and non-LTE models to the description of the radiative properties of highly-radiating z-pinch plasmas is emphasized. Two different approaches to the calculation of plasma resistance and their effects on line radiation mechanisms are analyzed.

PACS numbers: 52.58.Lq, 52.59.Qy, 52.25.Jm

I. INTRODUCTION

High energy density plasmas produced by varieties of wire array loads have been extensively studied for the past few years at the University of Nevada, Reno at the 1.7 MA Zebra facility (see, for example, Ref. [1]). Various modeling tools such as radiation MHD and WADM codes [2] and non-LTE atomic kinetic models [3–5] have been applied to analyze plasma dynamics and radiation features. Further progress in this direction can be achieved by amplification of existing numerical tools and deeper understanding of processes and effects directly affecting the plasma radiation features, such as the Ohmic plasma heating. Direct comparison of various approaches to calculate plasma ionization balance and plasma electric resistance seems to be a feasible way to achieve the aforementioned goals.

The radiation MHD code, applied in [2] to simulate precursor column dynamics, in its current state uses a simplified Saha–Boltzmann model [6] that calculates plasma ionization balance in the LTE (Local Thermodynamic Equilibrium) approximation. Plasma electric resistance and other kinetic transport effects (electron and ion thermal conductivities *etc.*) are calculated according to the Braginskii model [7, 8].

Calculations of plasma ionization balance and plasma electric resistance by the Saha and Braginskii models will be verified versus the calculations by suite of codes based on the average atom model [9], which is a quantum-mechanical version of the Temperature Dependent Thomas–Fermi Theory by Feynman, Metropolis and Teller [10]. The average atom model also exploits the LTE approximation to calculate plasma ionization balance.

In this paper the analysis of data produced by different models will be focused on low- Z Al, mid- Z Cu and higher- Z Mo plasmas in broad ranges of the electron temperature T_e and electron number density n_e . The upper band for T_e (300 eV for Al and Cu and 1000 eV for Mo) and the lower band for n_e (10^{20} cm⁻³ for Al and Cu and 10^{21} cm⁻³ for Mo) have been chosen because of their relation to the parameter range typically extracted from Al K-shell and Cu and Mo

L-shell spectroscopic modeling. It also should be noted here that this parameter range is beyond the conventional application of the average atom model, which is characterized by much lower temperatures (typically < 20 eV) and near-solid-state densities.

The models of ionization balance in plasma are described, compared and discussed in the second section of this paper. In addition, the mean ion charge calculations by two LTE models are verified versus the data produced by non-LTE atomic kinetic codes. In the third section of this paper the average atom and Braginskii models of plasma resistance are described and compared with each other. The role of the Ohmic heating of plasma in application to the radiative properties of z-pinch is also discussed. Concluding remarks are given in the fourth section of this paper.

II. COMPARISON OF LTE AND NON-LTE IONIZATION BALANCE MODELS

Since the times of the first theoretical works on plasma physics, the specific electric resistance of a plasma η is quite often calculated using the Spitzer formula [11]

$$\eta = \frac{1}{\sigma} = \frac{m_e \nu_e}{e^2 n_e}, \quad (1)$$

where σ is the specific plasma conductivity, m_e and e are the electron mass and electron charge, ν_e is the electron collision frequency, and n_e is the electron number density.

The number free charge carriers per unit volume of plasma n_e is defined by the plasma average charge \bar{Z}

$$n_e = \bar{Z} n_i = \bar{Z} \frac{\rho}{A m_u}, \quad (2)$$

where n_i is the ion number density, ρ is the plasma mass density, A is the atomic weight of plasma element, and m_u is the atomic mass unit. The mean ion charge \bar{Z} also affects the electron collision frequency ν_e and, thus, is very important for the calculation of plasma resistance.

In order to calculate the average charge of a plasma one has to use a specific ionization balance model, which defines the relation between \bar{Z} and the mass density ρ and electron temperature T_e of plasma. The most common assumption that is applied for various ionization models is the approximation of Local Thermodynamic Equilibrium (LTE). Two LTE models of plasma ionization balance will be considered below, then the results of these models will be compared with calculations by the suite of non-LTE atomic codes.

A. Generalized Saha equation for multiply charge ions

The generalized Saha equation for multiply charged ions [6] explores the LTE approximation and calculates the population of various ions in plasma. The following set of equations defines the ion population per unit volume:

$$n_e \frac{n_{m+1}}{n_m} = \frac{2}{h^3} (2\pi m_e T_e)^{3/2} \frac{u_{m+1}}{u_m} e^{-\chi_{m+1}/T_e}, \quad (3)$$

where n_m is the number density of the ions with the charge m , χ_{m+1} is the m th ionization potential (an electron transition from the ground state to infinity is assumed). The excitation multiplier (u_{m+1}/u_m) will be ignored in the calculation below for the sake of simplicity.

The system (3) contains Z equations and $Z + 2$ unknown variables (Z is the atomic number of plasma element) Two normalization equations

$$\sum_{m=0}^Z n_m = n_i = \frac{\rho}{Am_u} \quad \text{and} \quad \sum_{m=1}^Z mn_m = n_e \quad (4)$$

close the system of equations (3), while the value of mean ion charge \bar{Z} is provided by Eq. (2).

B. Average atom model

An average-atom model uses a central-field Schrödinger Equation

$$\left[\frac{p_e}{2m_e} - \frac{e^2 Z}{4\pi\epsilon_0 r} - eV(r) \right] \Psi_a(\mathbf{r}) = E\Psi_a(\mathbf{r}), \quad (5)$$

where p_e is the electron momentum. The index a is defined for bound $a = (n, l)$ and continuum $a = (E, l)$ states (here n and l are the quantum numbers). A self-consistent potential is

$$V(r) = V_{dir}(r) + V_{xc}(r), \quad (6)$$

where direct part is defined as

$$\nabla^2 V_{dir} = -\frac{e}{\epsilon_0} n_e(r) \quad (7)$$

with the electron density $n_e(r) = n_{eb}(r) + n_{ec}(r)$ from bound and free electrons respectively. The Kohn–Sham exchange

potential is expressed through the electron density in the following way:

$$V_{xc}(r) = -\frac{e}{4\pi\epsilon_0} \left[\frac{3n_e(r)}{\pi} \right]^{1/3}. \quad (8)$$

The bound-state contribution to electron density is

$$4\pi r^2 n_{eb}(r) = \sum_{n,l} \frac{2(2l+1)R_{nl}^2(r)}{1 + \exp([E_{nl} - \mu]/T_e)}, \quad (9)$$

where the radial wave function for bound electrons are normalized as

$$\int_0^\infty R_{nl}(r)R_{n'l}(r)dr = \delta_{nn'}. \quad (10)$$

The continuum contribution to the electron density is

$$4\pi r^2 n_{ec}(r) = \sum_l \int \frac{2(2l+1)R_{El}^2(r)}{1 + \exp([E - \mu]/T_e)} dE, \quad (11)$$

where the continuum functions are also normalized

$$\int_0^\infty R_{El}(r)R_{E'l}(r)dr = \delta(E - E'). \quad (12)$$

The normalization condition that Z electrons and the nucleus lie inside a neutral Wigner–Seitz sphere $r \leq r_0$

$$\int_0^{r_0} n_e(r) d^3\mathbf{r} = 4\pi \int_0^{r_0} n_e(r) r^2 dr = Z \quad (13)$$

leads to a value for the chemical potential μ .

Equations (5) to (13) above are solved self-consistently to give the potential V , the wave functions and the chemical potential. The continuum wave functions inside the Wigner–Seitz cell merge smoothly into phase-shifted free-electron wave functions outside the sphere. The free-electron density $n_e(r)$ function, which also converges smoothly to an r -independent constant for $r > r_0$ is related to the ion density by

$$n_{ec} = \bar{Z} n_i. \quad (14)$$

C. Comparison with non-LTE atomic model

The application of LTE approximation is justified in plasmas under certain conditions that require collisional transitions to dominate radiative transitions between states. Generally, these conditions are fulfilled in dense plasmas having a huge number (typically, more than a million) of collisions per radiative life-time. In this case the radiation field is relatively weak to affect noticeably the ionization and excitation equilibria.

For the plasma parameter range relevant to Zebra z-pinch the applicability of the LTE approximation is defined the rule of thumb

$$n_e \gg 10^{13} \text{ cm}^{-3} \left(\frac{T_e}{1 \text{ eV}} \right)^{1/2} \left(\frac{\Delta E}{1 \text{ eV}} \right)^3, \quad (15)$$

where ΔE is the typical energy scale associated with the electron transitions that can be roughly estimated through the ionization potential of hydrogen $I_H = 13.6 \text{ eV}$ and principal quantum number n as follows:

$$\Delta E \sim I_H \frac{Z^2}{n^2}. \quad (16)$$

If the condition (15) is not fulfilled, the LTE approximation, and particularly the Saha–Boltzmann approach used in Eq. (3), are no longer applicable.

The suite of non-LTE atomic codes has been applied below to calculate the ionization balance in Al, Cu and Mo plasmas. Energy levels, radiative and collisional rates with complete coupling between the levels were computed with the Flexible Atomic Code [12].

The non-LTE kinetic model of Al (see, for example, Ref. [3]) includes all ionization stages with a detailed structure. The most detailed atomic structure is introduced for H- to Li- like ions. In particular, singly excited states of H-like up to $n = 6$, He-like up to $n = 5$, Li like up to $n = 4$ were included. Calculations of the average ion charge \bar{Z} with non-LTE atomic codes are compared with the calculations by two LTE models (Saha and average atom models) in Fig. 1. We expect the non-LTE model to be the most accurate in calculations of \bar{Z} .

As we can see from the analysis of data in Fig. 1, despite the significant difference in approaches to calculate the average ion charge two LTE models reasonably agree with each other. At the same time the departure of LTE calculations from non-LTE model becomes quite significant for n_e below 10^{23} cm^{-3} , especially for the temperatures $T_e > 150 \text{ eV}$. This observation is in agreement with Eq. (15): for Al plasma at $T_e = 300 \text{ eV}$ ($\Delta E \approx 400 \text{ eV}$) there should be $n_e \gg 10^{23} \text{ cm}^{-3}$.

The accuracy of ionization balance calculations is the key factor in building an adequate radiation model of plasma. Data in Fig. 1 show that in lower temperature region $T_e < 100 \text{ eV}$ even at density $n_e = 10^{20} \text{ cm}^{-3}$ the departure of Saha model from non-LTE model is not yet critical. Implementation of the simplified Saha model in the radiation MHD code can still result in reasonable accuracy of the simulations. However, at temperatures higher than 150 eV Saha model leads to a significant overestimation of plasma radiation and underestimation of the electron temperature, which can dramatically alter the simulation results (see, for example, the discussion in Ref. [13]).

The Cu non-LTE kinetic model was previously developed to diagnose the L-shell radiation from Cu X-pinch and planar wire array loads. Briefly, the Cu kinetic model include the ground states from the bare to neutral atoms and the details from H- to Al-like ions, including singly and doubly

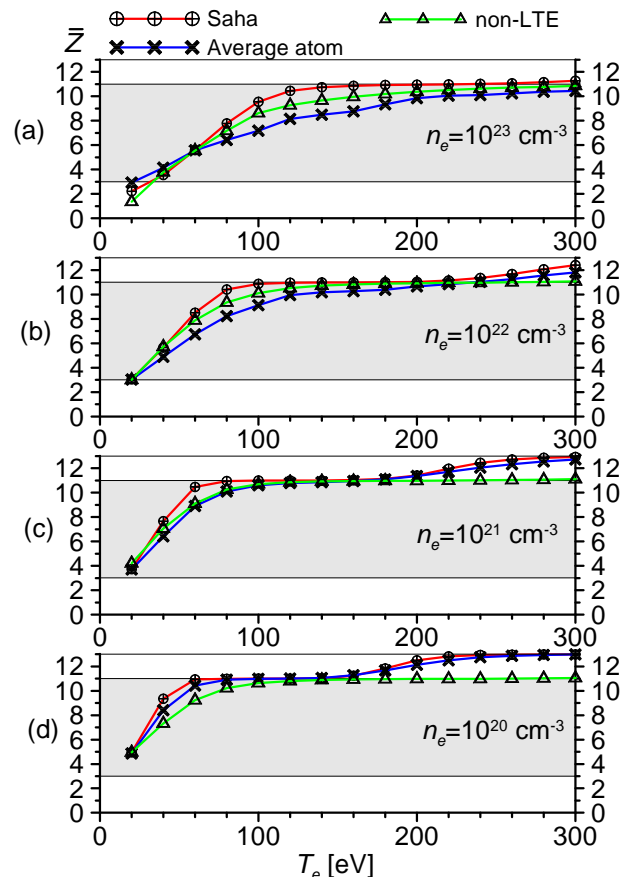


FIG. 1. (Color online) The average ion charge \bar{Z} of an Al plasmas as a function of electron temperature T_e calculated according to three different approaches at fixed electron densities: (a) $n_e = 10^{23} \text{ cm}^{-3}$, (b) $n_e = 10^{22} \text{ cm}^{-3}$, (c) $n_e = 10^{21} \text{ cm}^{-3}$ and (d) $n_e = 10^{20} \text{ cm}^{-3}$.

excited states. The singly excited states are included up to $n = 6$ for H-like ions, $n = 5$ for He- to Li-like ions and Ne- and Na-like ions, and $n = 4$ for Be- to F-like ions and Mg and Al-like ions. The doubly excited states include up to $n = 3$ for He-, Li-, Na-, Mg-, and Al-like ions and $n = 2$ for Be-like ions. More detailed description of this model can be found, for example, in Ref. [4]. Non-LTE calculations of the ionization balance in Cu plasma are compared with the results produced by two LTE models in Fig. 2 in the temperature range $20 \text{ eV} < T_e < 300 \text{ eV}$.

The analysis of the data in Fig. 2 reveals generally the same trends as for an Al plasma. The calculations of mean \bar{Z} ion charge by two LTE models reasonably agree with each other. Yet, as the value of the electron density drops from $n_e = 10^{23} \text{ cm}^{-3}$ to 10^{21} cm^{-3} the departure of LTE model calculations from non-LTE modeling becomes quite significant for higher temperatures $T_e > 150 \text{ eV}$. As we can see, at lower electron densities $n_e \leq 10^{20} \text{ cm}^{-3}$ the LTE approximation breaks down for the whole temperature range.

The Mo non-LTE kinetic and radiative model has been developed earlier to describe Mo L-shell radiation from X-pinch and planar wire arrays (see, for example,

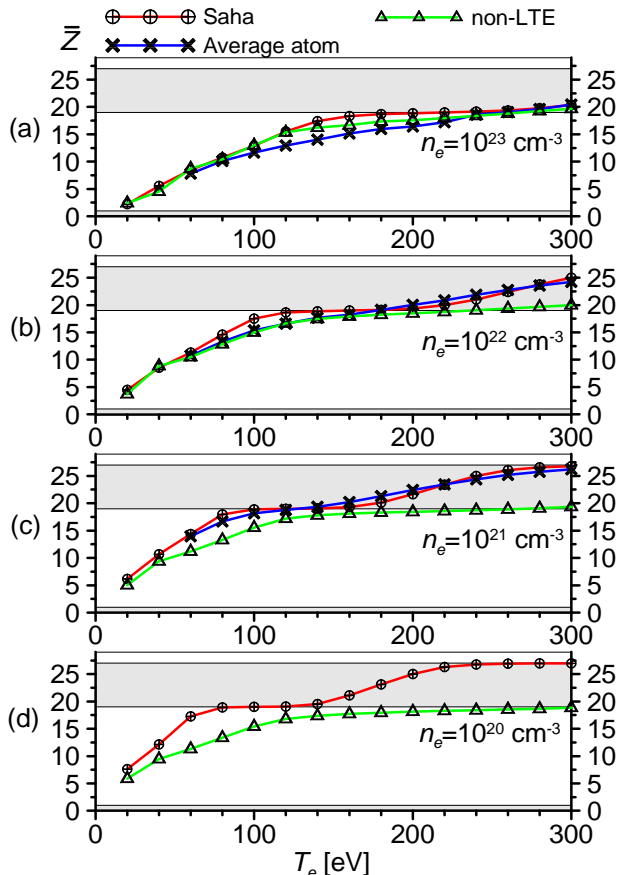


FIG. 2. (Color online) The average ion charge \bar{Z} of a Cu plasmas as a function of electron temperature T_e calculated according to three different approaches at fixed electron densities: (a) $n_e = 10^{23} \text{ cm}^{-3}$, (b) $n_e = 10^{22} \text{ cm}^{-3}$, (c) $n_e = 10^{21} \text{ cm}^{-3}$ and (d) $n_e = 10^{20} \text{ cm}^{-3}$.

Ref. [5]). Briefly, energy levels, spontaneous and collisional rates, collisional and photo ionization cross-sections were taken from a relativistic multi-configuration atomic structure code (HULLAC). The ground states of all ions from neutral to bare Mo configurations were considered. Detailed structure for O-like to Mg-like Mo ions included singly excited states up to $n = 7$ for O- through Ne-like ions, both singly and doubly excited states up to $n = 7$ and $n = 4$ for Na- and Mg-like ions. Calculations of the average ion charge \bar{Z} in Mo plasma by non-LTE kinetic model are compared with the results produced by two LTE models in Fig. 3. The temperature range for these calculations has been extended to 1000 eV.

As we can see from the analysis of the data presented in Fig. 3, two LTE models yield very close values of \bar{Z} for the whole temperature and density ranges. The departure of LTE models from non-LTE model becomes very significant, particularly for high-temperature range $T_e > 500 \text{ eV}$, as the electron density drops to $n_e = 10^{23} \text{ cm}^{-3}$. For lower electron densities the LTE approximation breaks down for the whole temperature range $50 \text{ eV} < T_e < 1000 \text{ eV}$.

By the analysis of the data presented in Figs. 1–3, one can

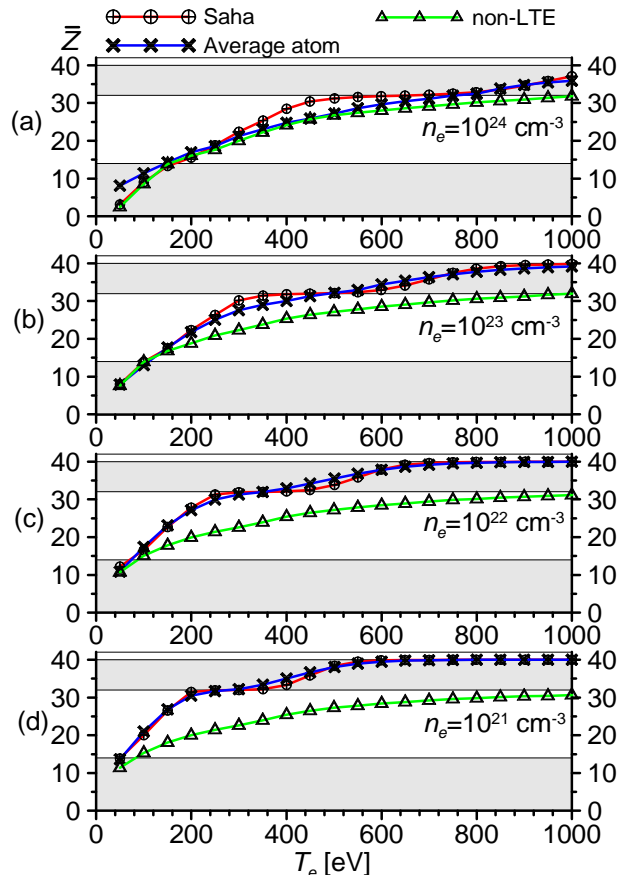


FIG. 3. (Color online) The average ion charge \bar{Z} of a Mo plasmas as a function of electron temperature T_e calculated according to three different approaches at fixed electron densities: (a) $n_e = 10^{24} \text{ cm}^{-3}$, (b) $n_e = 10^{23} \text{ cm}^{-3}$, (c) $n_e = 10^{22} \text{ cm}^{-3}$ and (d) $n_e = 10^{21} \text{ cm}^{-3}$.

see the general trend: as we move to heavier and higher- Z elements the applicability range of the LTE approximation shrinks dramatically in (n_e, T_e) parameter plane. The explanation lies in fact that plasmas composed of heavier elements have lesser ion number density and, thus, lower collision rate.

III. MODELS OF PLASMA ELECTRIC RESISTANCE

Below in this paper we discuss in greater details two approaches to the calculation of plasma electric resistance. Both these approaches use the same final formula, which is presented by Eq. (1), but have quite different methods of calculating the electron collision frequency ν_e .

A. Braginskii model

The analytic expression for the electron collision frequency had been provided in Braginskii's original work [7]. With

some amplifications performed in Ref. [8], the related equation is

$$\nu_e = \frac{1}{6\pi\sqrt{2\pi}} \frac{\bar{Z}^2 e^3 n_e}{\varepsilon_0^2 m_e^{1/2} T_e^{3/2}} \Lambda_e, \quad (17)$$

where Λ_e is the Coulomb logarithm, the special plasma parameter that was introduced to compensate the divergence of the integral of Coulomb potential

$$\Lambda_e = \frac{1}{2} \ln \frac{(12\pi)^2 \varepsilon_0^3 T_e^3}{e^2 n_e (1 + \bar{Z} T_e / T_i) (\bar{Z}^2 + \frac{3}{8} T_e / I_H)}, \quad (18)$$

The validity of the Braginskii model of plasma kinetic transport is justified until the mean free path of the electrons λ_e is much less than the typical spatial scale L of plasma system

$$\lambda_e = \frac{v_{Te}}{\nu_e} \ll L. \quad (19)$$

In the above equation $v_{Te} = \sqrt{3T_e/m_e}$ is the average thermal velocity of the electrons.

The value of the Coulomb logarithm can only be estimated, rather than derived exactly from basic plasma parameters. Depending on plasma conditions, the estimated value of Λ_e varies up to the order of its magnitude: $\Lambda_e \sim 2 - 20$. As we can see from Eqs. (1) and (17)–(18) the Coulomb logarithm is also a multiplicative factor in the expression for plasma electric resistance. This factor produces the major uncertainty in the Braginskii model.

B. Average atom model

In the average atom model the electron collision frequency is expressed through the momentum-dependent transport scattering cross-section σ_{tr} (see, for example, the discussion Ref. [9])

$$\nu_e = \frac{1}{\tau_e} = n_i v_F \sigma_{tr}, \quad (20)$$

where τ_e is the electron relaxation time, and v_F is the Fermi velocity of the electrons

$$v_F = \frac{p_e}{m_e}. \quad (21)$$

The transport scattering cross-section is expressed through the scattering amplitude f in the following way

$$\sigma_{tr} = \int (1 - \cos \theta) |f(\theta)|^2 d\Omega. \quad (22)$$

The scattering amplitude $f(\theta)$ in the above equation can be represented by the sum of partial waves

$$f(\theta) = \frac{\hbar}{4i\pi p_e} \sum_l (2l+1) (e^{2i\delta_l} - 1) P_l(\cos \theta), \quad (23)$$

where P_l is the Legendre polynomial, and δ_l is the scattering phase for the l th partial wave. Then, the equation for momentum-dependent transport cross-section becomes

$$\sigma_{tr}(p_e) = \frac{\hbar^2}{p_e^2} \sum_l \frac{2l+1}{\pi} \sin^2 \delta_l. \quad (24)$$

The momentum-dependent expression for static electric conductivity of plasma based on the arguments from kinetic theory is provided by Ziman formula

$$\sigma = \frac{2e^2}{3} \int \left[-\frac{\partial f}{\partial E} \right] \frac{v_F^2 \tau_e}{\hbar^3} d^3 p_e. \quad (25)$$

Momentum-independent expression for plasma resistivity is reduced to the Drude formula, which is exactly the same as the Spitzer formula given by Eq. (1).

C. Model comparison

The Braginskii model provides analytic expressions for the specific electric resistance of plasma η . According to Eqs. (1) and (17)

$$\eta \propto \frac{\bar{Z}^2}{T_e^{3/2}} \Lambda_e. \quad (26)$$

Thus, the specific electric resistance η should decrease with the increase of the electron temperature, and should have only a weak dependence on the electron density through $\bar{Z}(n_e, T_e)$ and $\Lambda_e(n_e, T_e)$.

The values of Al plasma electric resistance calculated according to the Braginskii and average atom models are compared in Fig. 4. As we can see, two models are quite in agreement for low-temperature and high-density limit $n_e \leq 10^{22} \text{ cm}^{-3}$ and $T_e < 50 \text{ eV}$. The discrepancy, however, becomes more significant at higher temperatures. Moreover, the average atom model does not reveal any significant resistance change with the variation of the electron density. The Braginskii model shows the slight increase of plasma electric resistance as the electron density decreases, giving an increase to mean ion charge \bar{Z} . With the decrease of electron density the departure of the Braginskii model from the average atom models increases.

Comparison of the calculations of plasma resistance by two models for Cu and Mo plasmas are shown in Fig. 5 and Fig. 6 respectively. Calculated values of electric resistance of Cu and Mo plasmas data on these figures generally repeat the same trends as the one observed for Al plasma resistance. Two models give close predictions at dense $n_e \leq 10^{22} \text{ cm}^{-3}$ lower temperature $T_e < 50 \text{ eV}$ plasma limit. The discrepancy between the two models increases with the increase of electron temperature and the decrease of electron temperature.

Thus, the Braginskii model predicts higher values of plasma electric resistance than the average atom model. At high-temperature $T_e \geq 300 \text{ eV}$ and low-density $n_e =$

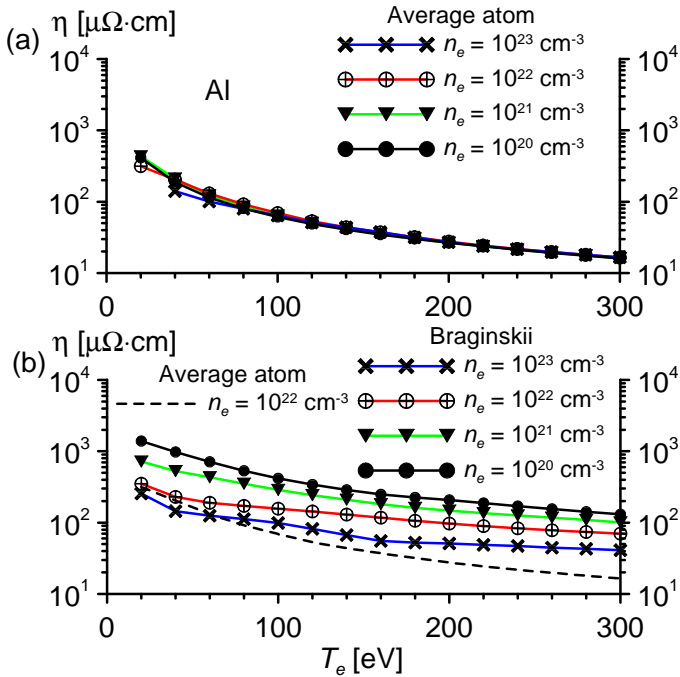


FIG. 4. (Color online) The electric resistance of Al plasma as a function of electron temperature at four given values of electron density $n_e = 10^{23}$, 10^{22} , 10^{21} and 10^{20} cm^{-3} calculated according to the average atom model (a) and Braginskii model (b).

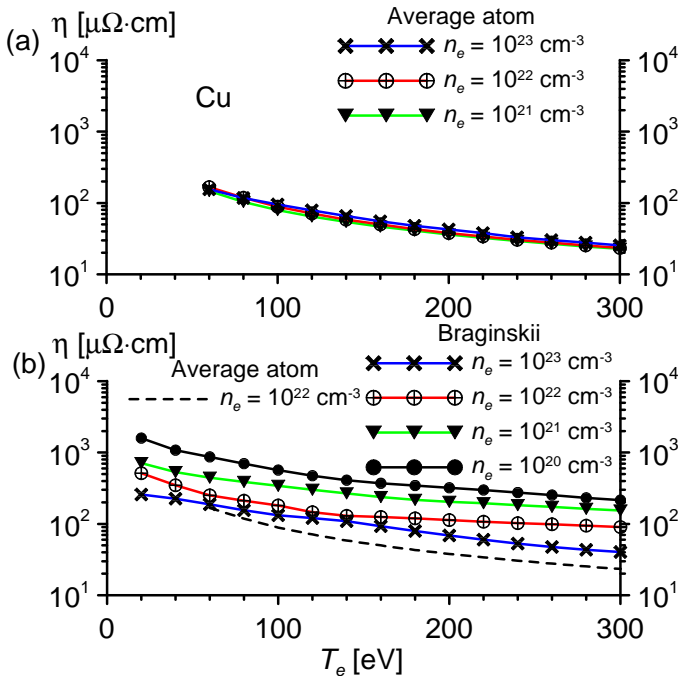


FIG. 5. (Color online) The electric resistance of Cu plasma as a function of electron temperature at four given values of electron density $n_e = 10^{23}$, 10^{22} , 10^{21} and 10^{20} cm^{-3} calculated according to the average atom model (a) and Braginskii model (b). Plasma resistivity at $n_e = 10^{20} \text{ cm}^{-3}$ calculated only by Braginskii model.

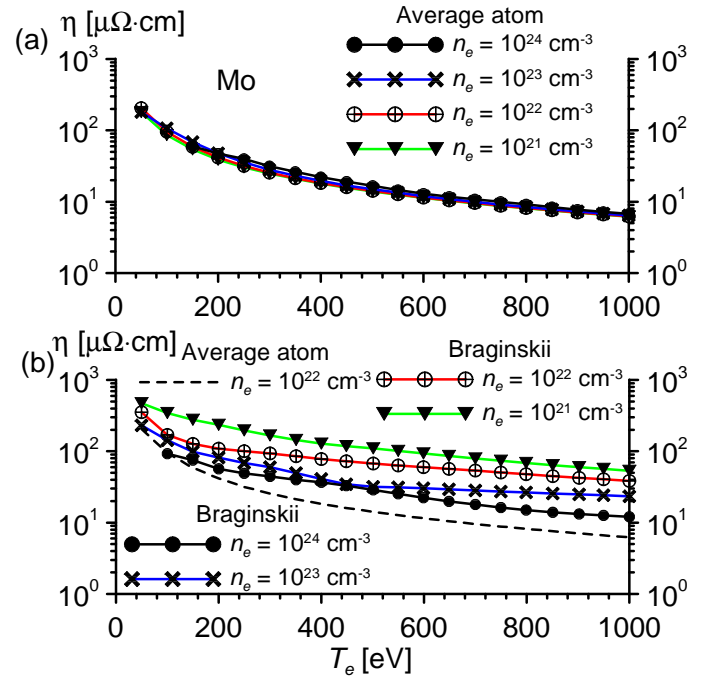


FIG. 6. (Color online) The electric resistance of Mo plasma as a function of electron temperature at four given values of electron density $n_e = 10^{24}$, 10^{23} , 10^{22} and 10^{21} cm^{-3} calculated according to the average atom model (a) and Braginskii model (b).

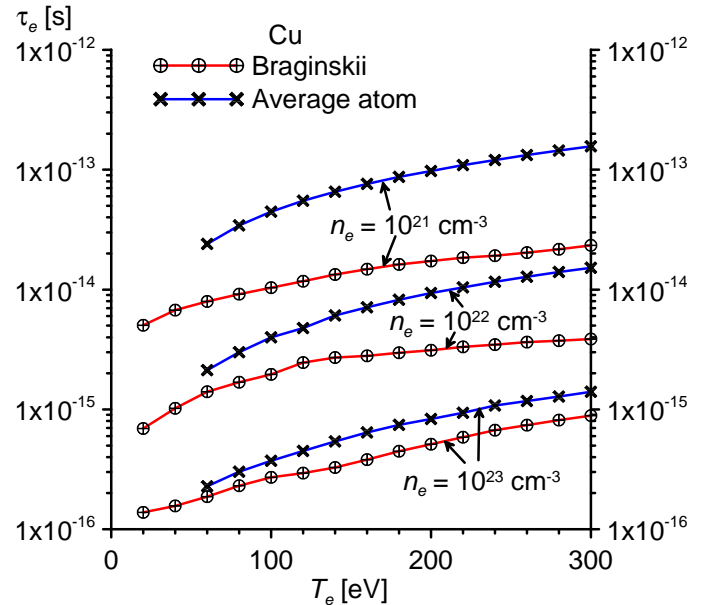


FIG. 7. (Color online) Electron relaxation time τ_e as a function of electron temperature T_e calculated for Cu plasma in Braginskii and average atom approximations at $n_e = 10^{21} \text{ cm}^{-3}$, $n_e = 10^{22} \text{ cm}^{-3}$, and $n_e = 10^{23} \text{ cm}^{-3}$.

10^{22} cm^{-3} limit the discrepancy of the predicted values of electric resistance is measured by the factor ~ 8 .

The discrepancy in calculations of η can be explained by the difference in approaches implemented in the Braginskii and average atom models to calculate the transport cross-section σ_{tr} (classic mechanical and quantum mechanical approaches respectively). In both models σ_{tr} can be expressed directly through the electron collision frequency as in Eq. (20) [v_F should be replaced by v_{Te} in Braginskii model]. Fig. 7 shows the electron relaxation time τ_e (the inverse of electron collision frequency $\nu_e = 1/\tau_e$) as a function of T_e calculated for Cu plasma according to the Braginskii and average atom models.

Although the calculation of the transport cross-section in the average atom model through the scattering amplitude $f(\theta)$ and summation over the partial waves is much more accurate than a classical mechanical approach in the Braginskii model, the applicability of the former model is mostly limited to the warm dense matter, which corresponds to the lower temperature $T_e < 50 \text{ eV}$ and higher density $n_e \geq 10^{22} \text{ cm}^{-3}$ limit in Figs. 4 to 7. At the same time, even at the most "collisionless" regime considered above (Mo plasma at $T_e = 1000 \text{ eV}$ and $n_e = 10^{21} \text{ cm}^{-3}$) the applicability condition for Braginskii model (19) gives $\lambda_e = 1.5 \mu\text{m} \ll L \sim 1 \text{ mm}$.

D. Applications to z-pinch physics

The electric resistance R of z-pinch of length l_z and radius r_p can be calculated as

$$R = \eta \frac{l_z}{\pi r_p^2}. \quad (27)$$

Fig. 8 presents the resistance of z-pinch as a function of electron temperature for Al, Cu and Mo plasmas at $n_e = 10^{21} \text{ cm}^{-3}$ and assuming $l_z = 20 \text{ mm}$ and $r_p = 0.5 \text{ mm}$. As we can see from the analysis of the data in this figure, the values of the electric resistance depend weakly on the chemical element chosen, but have stronger dependence on the value of electron temperature.

Typical electron temperatures of Cu plasma are estimated for L-shell line radiation to be in the range 300–350 eV (see, for example, Ref. [4]). According to Fig. 8, at the temperature $T_e = 300 \text{ eV}$ a uniform Cu plasma column would have an electric resistance $R_A = 6 \text{ m}\Omega$ according to the average atom model and $R_B = 45 \text{ m}\Omega$ according to the Braginskii model.

The rate of the Ohmic heating of plasma column P can now be estimated as

$$P = RI^2, \quad (28)$$

where I is the total electric current through the column. Taking the maximum current $I = 1 \text{ MA}$, we get the estimation for the Ohmic heating rate $P_A = 6 \text{ GW}$ and $P_B = 45 \text{ GW}$ in average atom and Braginskii approaches respectively. Assuming the x-ray pulse duration $\sim 10 \text{ ns}$, we get the following estimation for the energy of the Ohmic heating of plasma:

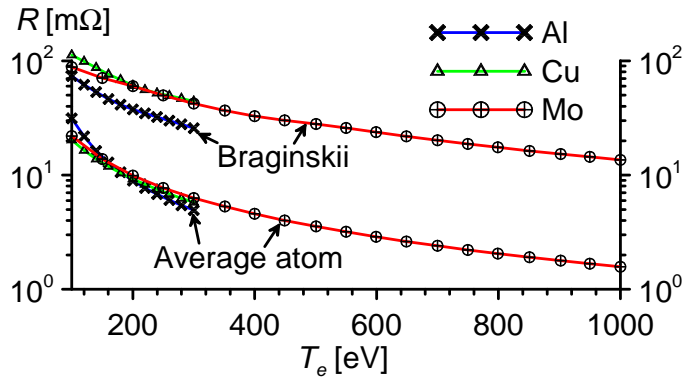


FIG. 8. (Color online) Electric resistance R of z-pinch calculated for Al, Cu and Mo plasmas according to the Braginskii and average atom approximations at $n_e = 10^{21} \text{ cm}^{-3}$ and assuming $l_z = 20 \text{ mm}$ and $r_p = 0.5 \text{ mm}$ [Eq. (27)].

$W_{\Omega A} \approx 60 \text{ J}$ and $W_{\Omega B} \approx 450 \text{ J}$. The number produced in Braginskii model is quite close to the total line radiation energy measured in experiments with Cu z-pinch [14]. Thus, according to the Braginskii model the Ohmic heating may contribute significantly into the energy balance of line radiation plasma sources. According to the average atom model this contribution is not significant.

The electron temperature of Mo plasma has been estimated from L-shell spectroscopic modeling (see, for example, Ref. [5]) to be in the range 1000–1500 eV. At temperature $T_e = 1000 \text{ eV}$ according to the data in Fig. 8 the resistance of plasma column is $R_B = 14 \text{ m}\Omega$, which leads to $P_B = 14 \text{ GW}$ and $W_{\Omega B} \approx 140 \text{ J}$. Thus, according to the Braginskii model, the relative contribution of Ohmic heating into the energy balance of line radiation plasma sources diminishes as we move toward higher- Z elements having higher L-shell radiation temperatures. The average atom model predicts negligibly low values of Mo plasma column resistance $R_A = 1.6 \text{ m}\Omega$ and the Ohmic heating energy $W_{\Omega A} \approx 16 \text{ J}$.

The average atom and Braginskii models of plasma electric resistance agree that the Ohmic heating rate in z-pinch plasma is not enough to explain the generation of the main x-ray bursts with powers up to 1 TW and the total radiated energies $> 20 \text{ kJ}$ [1]. Hence, the classic electric resistance models, discussed in details in this paper, cannot explain an excess amount of total radiated energy over the thermalized kinetic energy, which typically is 4–8 kJ [15]. The mechanism of plasma heating that can be responsible for the main x-ray burst generation is generally referred to as an "anomalous plasma heating" (see, for example, Ref. [16]). This mechanism should have an intensity of at least one order of magnitude higher than the classic one, based on kinetic transport in plasma and accounted by the average atom and Braginskii models.

IV. CONCLUSION

The two LTE models, the average atom model and the Saha–Boltzmann model, produce quite close results for the mean ion charge of plasma \bar{Z} in a wide range of temperatures and densities considered in this paper. The expected departure of LTE models from non-LTE model increases with the increase of the electron temperature T_e and decrease of the electron number density n_e for all three elements considered: Al, Cu and Mo. In the same parameter range the discrepancy between LTE and non-LTE models becomes more pronounced for higher- Z elements. Being implemented in the radiation MHD codes, non-LTE model is expected to produce the most accurate results.

The average atom model is expected to be the most accurate in calculation of plasma electric resistance in warm-dense-matter limit $T_e < 20$ eV and $n_e \geq 10^{23}$ cm $^{-3}$. In this parameter range the values of the electric resistance are very close to those produced by the Braginskii model. As the elec-

tron temperature increases and the electron number density decreases, the divergence between two becomes more significant. For the parameter range that mostly corresponds to plasma L-shell radiation ($n_e \leq 10^{21}$ cm $^{-3}$, $T_e \sim 300$ eV for Cu and $T_e \sim 1000$ eV for Mo) this divergence is accounted for by a factor ~ 8 . The average atom and Braginskii models predict the decrease of Ohmic heating intensity for higher- Z plasmas. Both models of plasma electric resistance agree that the Ohmic heating mechanisms based on the kinetic transport in plasma is not intense enough to affect the power balance of the main x-ray burst.

ACKNOWLEDGMENTS

Authors greatly appreciate fruitful discussions with A. Velikovich, L. Rudakov, S. Hansen, D. Ampleford, C. Coverdale, N. Pereira, P. Sasorov and N. Bobrova.

This work was supported by NNSA under DOE Cooperative Agreements DE-FC52-06NA27588 and part by DE-FC52-06NA27586.

-
- [1] V. L. Kantsyrev, A. S. Safronova, A. A. Esaulov, *et al.*, HEDP **5**, 115 (2009).
 - [2] A. A. Esaulov, V. L. Kantsyrev, A. S. Safronova, *et al.*, HEDP **5**, 166 (2009).
 - [3] A. S. Safronova, V. L. Kantsyrev, A. A. Esaulov, *et al.*, Phys. Plasmas **15**, 033302 (2008).
 - [4] N. D. Quart, A. S. Safronova, V. L. Kantsyrev, *et al.*, IEEE Transactions on Plasma Science **38**, 631 (2010).
 - [5] M. F. Yilmaz, A. S. Safronova, V. L. Kantsyrev, *et al.*, JQSRT **109**, 2877 (2008).
 - [6] Ya. B. Zeldovich and Yu. P. Raizer, *Physics of shock waves and high-temperature hydrodynamic phenomena*. Edited by W. D. Hayes and R. F. Probstein, New York, Academic Press, 1966–67.
 - [7] S. I. Braginskii, in *Plasma Physics and the Problem of Controlled Thermonuclear Reactions*, edited by M. A. Leontovich (Pergamon, New York, 1961), Vol. I, p. 135.
 - [8] N. A. Bobrova and P. V. Sasorov, Sov. J. Plasma Phys. **19**, 406 (1993).
 - [9] W. R. Johnson, HEDP **5**, 61 (2009).
 - [10] R. P. Feynman, N. Metropolis and E. Teller, Phys. Rev. **75**, 1561 (1949).
 - [11] L. Spitzer, *Physics of fully ionized gases*, 2nd edition, New York: Interscience, 1962.
 - [12] M. F. Gu, Can. J. Phys. **86**, 675 (2008).
 - [13] A. Esaulov, Phys. Plasmas **13**, 042506 (2006).
 - [14] A. S. Safronova, A. A. Esaulov, V. L. Kantsyrev, *et al.*, HEDP **7**, 252 (2011).
 - [15] A. A. Esaulov, V. L. Kantsyrev, A. S. Safronova, *et al.*, Phys. Plasmas **15**, 052703 (2008).
 - [16] A. A. Esaulov and P. V. Sasorov, Plasma Phys. Rep. **23**, 576 (1997).